Acta Oceanol. Sin., 2017, Vol. 36, No. 4, P. 13–20
DOI: 10.1007/s13131-017-0973-7
http://www.hyxb.org.cn
E-mail: hyxbe@263.net

Analysis of the characteristics of offshore currents in the Changjiang (Yangtze River) estuarine waters based on buoy observations

LI Peng[1], SHI Benwei[2]*, WANG Yaping[2], QIN Weihua[3], LI Yangang[1], CHEN Jian[1]

[1] Forecast Center for East China Sea, State Oceanic Administration, Shanghai 200136, China

[2] Ministry of Education Key Laboratory for Coast and Island Development, Nanjing University, Nanjing 210093, China

[3] Marine Environment Investigation Center of East China Sea, State Oceanic Administration, Shanghai 200137, China

Received 18 December 2015; accepted 20 June 2016

Abstract

A buoy of 10 m in diameter was used to record the current speed and direction in a vertical profile in the offshore area of the Changjiang (Yangtze River) Estuary (with an average water depth of 46.0 m) for one year. The results include: (1) the currents rotate clockwise and the current direction is consistent in a vertical profile without clear seasonal variations. (2) The horizontal current speeds are generally high, with a maximum of 128.5 cm/s occurring in summer and 105.5 cm/s appearing in winter commonly close to the surface. The average current speeds in the vertical profile fall in the same range (the differences are less than 8.0 cm/s), with the maximum of 47.0 cm/s occurring in summer and 40.8 cm/s in winter. The average current speed during spring tides is twice that during neap tides (26.5 cm/s). (3) Significant differences of speeds are observed in the vertical profile. The maximum current speed occurs at either surface (spring and winter) or sub-surface (summer and autumn), with the minimum current speed appearing at the bottom. The maximum average current speed of all layers is 57.9 cm/s, which occurs in the 18-m layer during summer. (4) The average speed of the residual currents ranges from 7.5 cm/s to 11.3 cm/s, with the strongest occurring in spring and weakest in winter. The residual currents of all layers are eastward during spring and winter, whereas northeastward or northward during summer and autumn. (5) The currents in the offshore of Changjiang Estuary are impacted collectively by diluted Changjiang River discharge, the Taiwan Warm Current, monsoon and tides.

Key words: ocean currents, buoy observation, seasonal variations, Changjiang (Yangtze River) Estuary

Citation: Li Peng, Shi Benwei, Wang Yaping, Qin Weihua, Li Yangang, Chen Jian. 2017. Analysis of the characteristics of offshore currents in the Changjiang (Yangtze River) estuarine waters based on buoy observations. Acta Oceanologica Sinica, 36(4): 13–20, doi: 10.1007/s13131-017-0973-7

1 Introduction

Offshore currents play a key role in the movement of terrigenous oceanic material and a sound knowledge of the temporal and spatial variations of offshore currents is important to better understand environmental conditions, eutrophication problems and fishing activities in offshore sea regions (Rabouille et al., 2008; Tang et al., 2008). The currents in the offshore regions of the Changjiang (Yangtze River) Estuary are mainly affected by diluted water from the Changjiang River, the Taiwan Warm Current, the Subei coastal current, and the Zhejiang coastal current. Discharge from the Changjiang River is high and exhibits large seasonal variations (893×10^9 m^3/a; during the period of 1951–2013, the runoff flux between May and October accounted for 70% of the annual flux) (Dai et al., 2008, 2011a). Consequently, its expanding pattern is characterized by great intra- and inner-annual variations (Lie et al., 2003) that significantly affect the flow field of the offshore ecological environment and marine productivity (Zhu et al., 2005; Chang et al., 2014; Wu et al., 2014; Zhang et al., 2014). During summer, the diluted runoff from the Changjiang River can reach as far as the Jeju Island in Korea (Isobe et al., 2002; Senjyu et al., 2006; Moon et al., 2009). Thus, the Changjiang River greatly impacts the ecology of this sea region (Dai et al., 2010, 2011b). Because of the complex dynamic environment, a number of studies have been based on temperature and salinity data or numerical simulations to compensate for the lack of measured flow speeds (Chen et al., 2006; Moon et al., 2009; Park et al., 2011; Chang et al., 2014). Previous studies of the diluted Changjiang River discharge mainly focused on the water's expanding path and turning mechanisms (Mao et al., 1963; Lie et al., 2003; Huang et al., 2008; Wen et al., 2014). Long-term salinity data indicated that variations in the Zhejiang coastal current, Taiwan Warm Current and Changjiang River discharge are important factors in determining the turning direction of the diluted Changjiang River discharge (Liao et al., 2001). Zhu et al. (1997, 1998) and Liu et al. (2013) discussed the dynamics of the water by conducting numerical simulations to analyze the effects of external conditions, including the Taiwan Warm Current, runoff flux, wind field, Yellow Sea cold vortex and Subei coastal current on the expansion of the diluted Changjiang River discharge. Zhao (1991) proposed that the expansion of the Changjiang River

Foundation item: The Major State Basic Research Development Program under contract No. 2013CB956502; the State Key Laboratory of Estuarine and Coastal Research Funds under contract No. SKLEC200906; the National Natural Science Foundation of China under contract No. 41625021.

*Corresponding author, E-mail: shibenwei@126.com

discharge, invasion of the Taiwan Warm Current and spatial variations in wind stress predominate the expansion of the diluted water and turning mechanism. Using remote sensing technology, Pu et al. (2002) and Kim et al. (2009) studied weekly, ten-day and seasonal variations in the expansion directions of the diluted Changjiang River discharge and noted the limitations of studying the expansion mechanism based on large-scale observational data. However, almost all of these results are obtained from numerical simulations, short-term observational data and remote sensing. Sufficient hydrodynamic observations in particular, the long-term, continuous, fixed-point observational data, are not available in this region. In this study, we conducted continuous observations of currents in a vertical profile (fixed point) of the offshore region of the Changjiang Estuary (from August 1, 2006 to July 31, 2007 with a 10-m-long marine buoy to obtain a better understanding of the offshore currents of the Changjiang Estuary with the real-time data.

2 Regional setting

The study is focused the subaqueous delta on the offshore region of Changjaing Estuary, which is characterized by meso and regular semidiurnal tides. The offshore current in this area transitions from an alternating to rotational current moving in a clockwise direction (Chen et al., 1988). In winter, under the impact of strong winter monsoons, runoff has small flux amplitude and starts to move southward along the coast soon after it merging with the sea. In contrast, in summer, runoff leaving the estuary is moved by inertia southeastward as a “shooting current” or “quasi shooting current”. 20 to 60 km from the estuary, the runoff move northeastward and form a tongue-shaped expansion toward the Jeju Island to the northeast (Zhao, 1991; Su, 2005). In addition to the diluted Changjiang River discharge, the offshore currents of the Changjiang Estuary also include the Taiwan Warm Current, Zhejiang-Fujian coastal currents and Yellow Sea coastal current. The filtered tidal current speed caused by the diluted Changjiang River discharge, coastal current caused by monsoons, Kuroshio Current, and Taiwan Warm Current is 10–50 cm/s, and the residual current displays both spatial and seasonal variations (Zhu et al., 2004a, b). The Taiwan Warm Current on the west side of the East China Sea is the primary flow system that affects the East China Sea, and it moves northward at 50–100 m isobaths throughout the year and is stronger during summer and weaker during winter, with a speed of 15–40 cm/s; when it reaches the far shore of the Changjiang River, it decreases to 10–20 cm/s (Guan, 1978; Su and Pan, 1989). Under the combined influence of the Taiwan Warm Current and terrain, an apparent upwelling occurs with a speed of approximately 1.0×10^{-3}–5.0×10^{-3} cm/s (Zhao, 1993). Furthermore, the offshore portion of the Changjiang Estuary features large oxygen depletion areas whose positions are affected by variations in the circulation of adjacent sea regions and water masses (Li et al., 2002).

3 Data and methods

The observation station (31.25°N, 123.5°E) is located offshore of the Changjiang Estuary (Fig. 1) in an area with an average water depth of 46.0 m. From August 1, 2006 to July 31, 2007, we used a 10-m marine observational buoy for continuous observations of vertical currents, wind speed and direction, and waves. With a displacement of 50.4 tons, the diameter and height of the buoy are 10.0 m, with 0.9 m of the buoy sitting below the waterline. The buoy uses a single-point mooring (Fig. 1). A Doppler current profiler (500 kHz Acoustic Doppler Profiler (ADP), SonTek, USA; observational factors are current speed and direction) is installed on the bottom of the buoy and the sensor is extended for 0.3 m from the buoy floats (Fig. 1). The buoy’s observational system sways with waves and surface currents. The ADP data playback indicated that the equipment was well positioned during the observation period and that the inclination angles in the X and Y directions were both smaller than 5°. The blanking distance of the ADP instrument is 1.0 m, the sampling averaging interval is 10 min, the sampling duration is 1 min, the cell size is 8.0 m, and the number of cells is set at eight. According to the sensor’s installation depth and blanking distance, the calculated depth of the first layer is 10.0 m (10.0 m is used here for calculations and descriptions for simplicity, rather than the exact number that was calculated as 10.2 m). The intensity of sound signal in the ADP allowed us to infer that there are five effective observational layers (10.0 m, 18.0 m, 26.0 m, 34.0 m and 42.0 m; the sensor can only detect sub-surface to sub-bottom sea currents, yet, the surface and bottom cannot be detected). The wind speed and direction

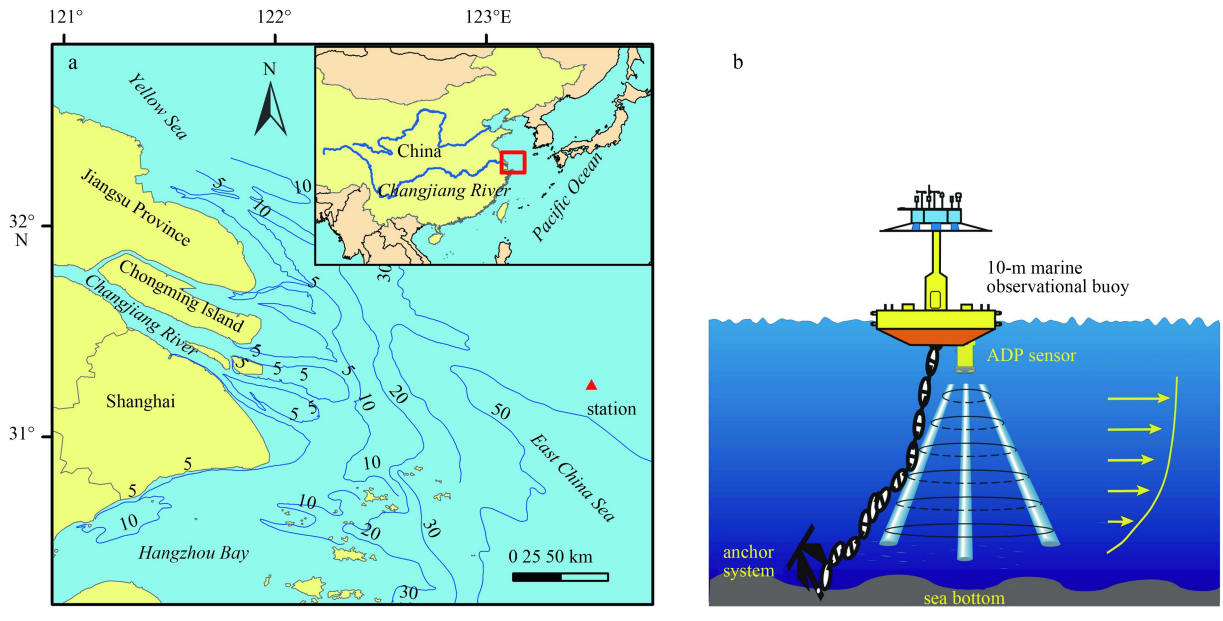

Fig. 1. Observational position (a) and buoy (ADP) working (b) illustrations.

are measured using a 05103 anemometer by Young Enterprises, USA. An anemometer is installed on the equipment platform on top of the buoy (10.0 m from the sea surface), and winds are sampled every three hours; when the average wind speed is greater than 10 m/s, the sampling interval is shortened by 1 h. In addition, surface salinity data have been obtained for this station from July 2009 to October 2010 (the sampling interval is 1 h, the equipment model is COMPACT-DT).

The sensors on the buoy automatically measured data, which are transferred to the coastal station (Forecast Center for East China Sea, State Oceanic Administration) via the Inmarsat-C satellite (the ADP memorizer automatically backs up the data). To analyze the seasonal variation of the sea currents, we selected the months of April, July, October and January to represent spring, summer, autumn and winter, respectively. Calculations are based on the average of two spring tides and two neap tides each month. The Changjiang River runoff flux information was obtained from the Yangtze River Water Resources Committee.

4 Results

4.1 *Current speed and direction*

This station is located in the open sea region of the Changjiang Estuary. The sea current is discovered to rotate clockwise. The current direction is consistent along the vertical direction without obvious seasonal variation, as illustrated in Figs 2–5 (For the sake of clarity to display the speeds and directions of currents, only the transitions from spring to neap tides are plotted in the figures. The data interval is 30 min).

The horizontal current speeds in the offshore region of the Changjiang Estuary are found generally high. Table 1 shows that the vertical average current speed varies little with time (the differences are less than 8.0 cm/s). The maximum current speed of 47.0 cm/s occurs in summer, whereas 40.8 cm/s occurs in winter. The maximum current speeds during all seasons are higher than 100.0 cm/s; the maximum current speed during summer can reach 128.5 cm/s, whereas the maximum current speed during winter is relatively slow (105.5 cm/s). The maximum current speeds during all four seasons occur at the surface (at the 10-m layer). The average current speed during spring tides reaches its maximum during autumn (60.5 cm/s), whereas the average current speed during neap tides reaches the maximum during summer. The average current speeds during spring tides are approximately 1.7 to 3.0 times those during neap tides. In the vertical direction, the maximum current speeds during all seasons are the lowest on the bottom and the highest on the surface (during the observation period); therefore, the current speeds increase from the bottom to the surface. The maximum current speeds of the bottom layer range from 46.5 cm/s (winter) to 60.3 cm/s (spring), and the maximum current speeds on the surface range

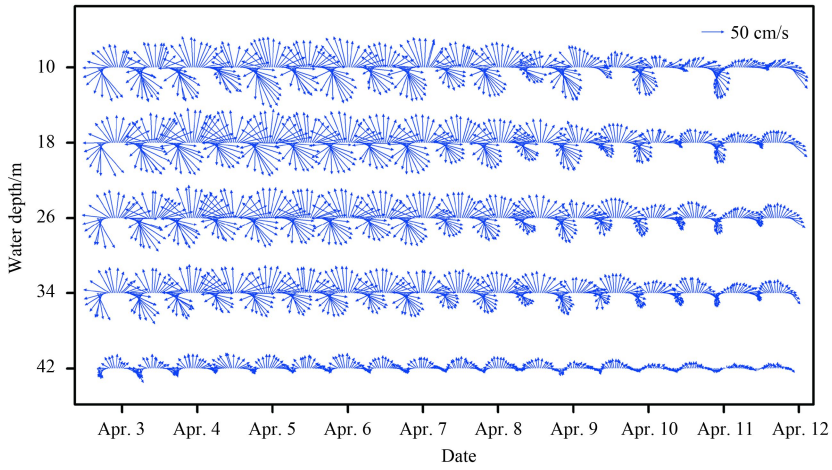

Fig. 2. Temporal variations in the current vectors during spring.

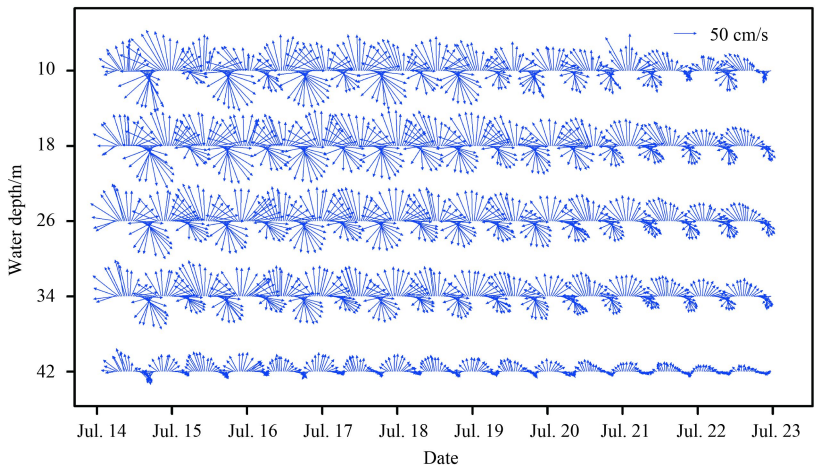

Fig. 3. Temporal variations in the current vectors during summer.

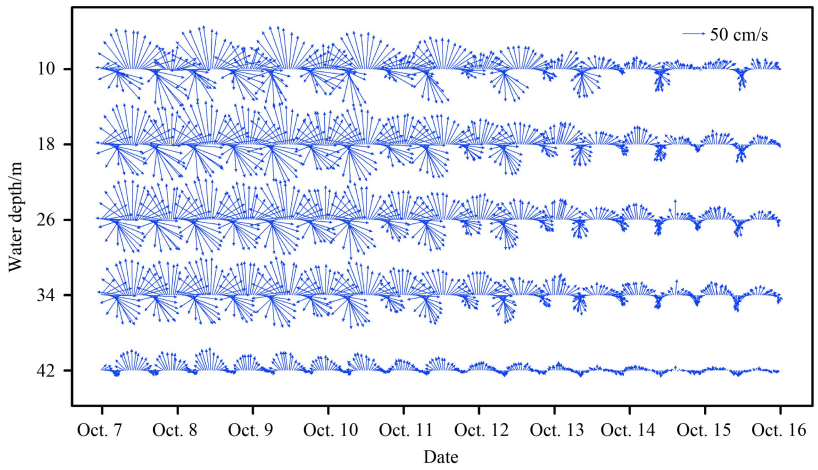

Fig. 4. Temporal variations in the current vectors during autumn.

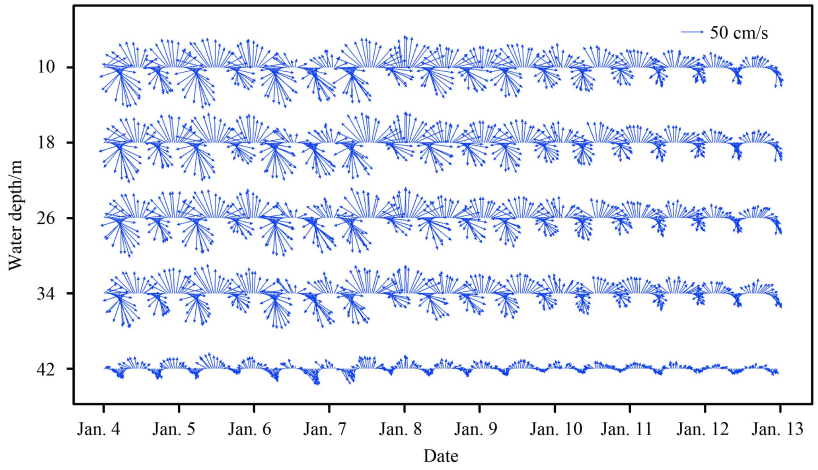

Fig. 5. Temporal variations in the current vectors during winter.

Table 1. Characteristic average current speeds (cm/s) in the vertical profile

Time	Monthly average	Maximum	Minimum	Spring tide average	Neap tide average
Spring	42.9	120.4	1.4	53.9	25.3
Summer	47.0	128.5	1.6	56.0	32.4
Autumn	41.4	113.8	0.8	60.5	20.3
Winter	40.8	105.5	1.1	49.2	27.9

from 105.5 cm/s to 128.5 cm/s. The minimum current speeds are all lower than 10.0 cm/s, and significant differences are not observed among layers and seasons.

Considerable differences occur in the vertical average of current speeds in different layers and seasons (Fig. 6). During spring, the current speed is at its minimum on the bottom along the vertical direction (16.9 cm/s) and quickly increases from the bottom layer to the 34-m layer; above 26 m, the current speeds are generally the same (49.7–51.6 cm/s). The vertical curve of the current speeds during spring tides has a convex shape: the current speed is the lowest on the bottom and the highest in the 18-m layer (67.7 cm/s). During neap tides, the current speed is minimum on the bottom and maximum on the surface whereas the current speeds in the middle layers are relatively stable (current speeds of the 18–34 m layers range from 26.9 to 29.2 cm/s). The average current speeds during spring tides in the corresponding layers are 1.8 to 2.4 times those during neap tides, and the vertical average of current speeds is 2.1 times that during neap tides. The vertical sectional profile of current speeds during summer (the monthly average, spring-tide and neap-tide values) has a pronounced convex shape. The minimum current speeds in different periods all appear in the bottom layer (the monthly average, spring and neap values are 20.2, 26.7 and 13.0 cm/s, respectively), whereas the maximum current speeds are all in the middle-upper layers (the monthly, spring and neap values of the 18-m layer are 57.9, 67.2 and 40.5 cm/s, respectively). The current speeds of the surface and middle layers are generally the same. The vertical average of current speeds during spring tides is 1.7 times that during neap tides. During autumn, the monthly average current speed is the lowest on the bottom and the highest in the middle-upper layer (18-m layer; 54.2 cm/s), and the spring-tide curves clearly display a convex shape in the vertical direction. The highest current speed of the middle-upper layer can reach 75.0 cm/s. During neap tides, the current speed reaches its minimum on the bottom and is stable above the 34-m layer (22.7–23.7 cm/s). During winter, the current speed during spring tides is sig-

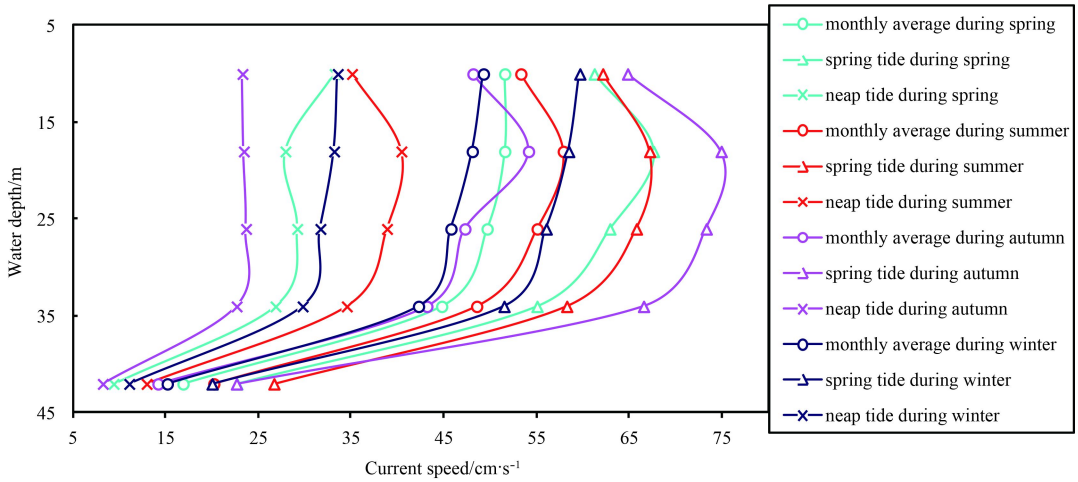

Fig. 6. Vertical variations in average current speeds during the observation period.

nificantly higher than that during neap tides, and the average current speed during spring tides is three times that during neap tides. During winter, the current speed is the lowest on the bottom and is stable above the middle layer; the average speeds during spring and neap tides are 49.2 and 27.9 cm/s, respectively, and the average current speeds during spring tides in the corresponding layers are 1.73 to 1.8 times those during neap tides. In general, the average current speed of the middle-upper layers is approximately 3.0 times that of the bottom layer. Except for the bottom layer, the current speeds of the corresponding layers are strongest during summer and weakest during winter; the average current speed during spring tides is strongest during autumn and weakest during winter; and the average current speed during neap tides is strongest during summer and weakest during autumn.

4.2 *Residual current*

During our observation period in the offshore region of the Changjiang Estuary, the residual current was strongest (13.5 cm/s) during summer and weakest (7.3 cm/s) during winter. The current speeds during spring and autumn were 10.8 cm/s and 9.9 cm/s, respectively. The current moved northeastward during summer and autumn (47.8° and 59.4°) and eastward during spring and winter (76.5° and 86.4°).

Apparent seasonal differences are observed in the residual currents in this sea region (Fig. 7). The residual currents were relatively strong during spring (Fig. 7). The vertical speed average was 11.3 cm/s during the observation period, and the current speed reached the maximum on the surface (14.5 cm/s) and decreased from the surface to the bottom (5.1 cm/s). The surface residual currents moved eastward (94.1°), and the residual currents shifted gradually counterclockwise from the surface to the bottom, where the current direction was 38.6°. During this period, the surface current directions during spring and neap tides shifted east by south, and those of other layers shifted east by north. In all layers, the currents during spring tides were shifted counterclockwise by 15° relative to that during neap tides. The vertical average of current speeds during spring tides was 12.9 cm/s, 1.6 times that during neap tides. Except for the consistent surface current speeds, the current speeds in the corresponding layers during spring tides were 1.6 to 2.5 times those during neap tides.

The residual currents during summer were strongest. The vertical average of current speeds was 13.6 cm/s, reaching the

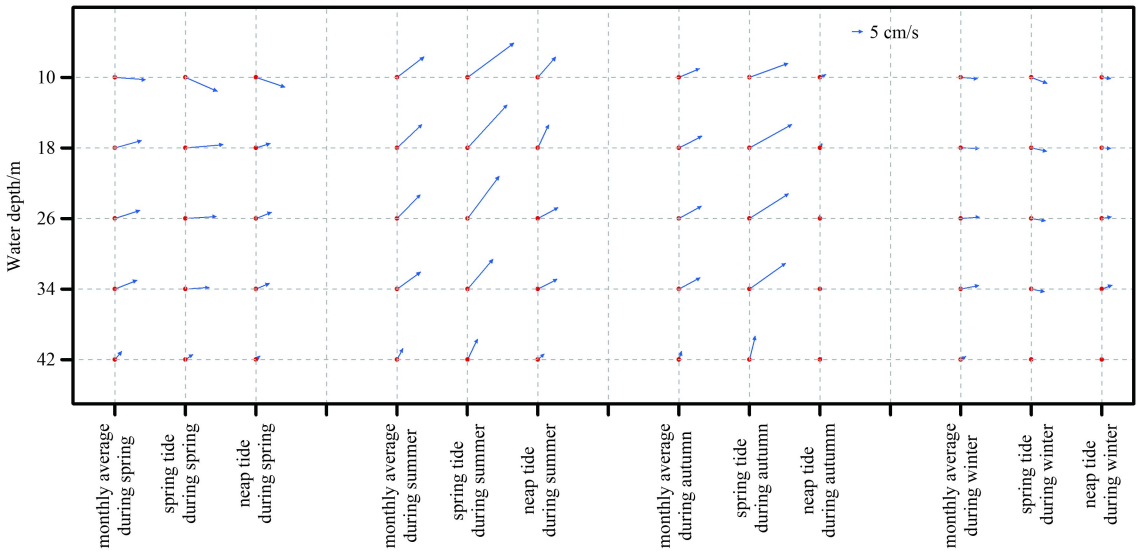

Fig. 7. Vertical variations in residual currents during the observation period.

maximum 16.1 cm/s in the middle-upper layer (18-m layers) and gradually decreased toward the bottom layer to 6.0 cm/s. The residual currents all moved northeasterly with a consistent speed above the 34-m layer (44.3° to 53.1°). The currents moved slightly northward in the bottom layer (28.1°). During spring and neap tides, the directions of residual currents were both northeastward; in the middle-upper layers (the 10-m and 18-m layers), the residual currents during spring tides shifted clockwise by approximately 15° relative to those during neap tides. In the middle-lower layers (below the 26-m layer), the residual currents during spring tides shifted counterclockwise by approximately 23° relative to those during neap tides. The residual currents during spring tides were strong and significantly higher than those during neap tides. The vertical average of current speeds during spring tides reached 21.9 cm/s, 2.2 times faster than that during neap tides. For the corresponding layers, the current speeds during spring tides were 1.8 to 2.6 times those during neap tides.

The vertical average of current speeds during autumn was 10.2 cm/s. The speeds of the residual currents were similar above the 34-m layer (10.8 to 12.3 cm/s). The current speed on the bottom was slow (4.2 cm/s). During autumn, the current speed during spring tides was fast, and the average current speed reached 19.4 cm/s (nearly that during spring tides during summer); the current speed on the bottom also reached 11.5 cm/s. The residual currents during neap tides were weak, and their speeds ranged from only 0.5 to 3.3 cm/s. Except for the bottom layer where there are northward-moving residual currents, all the residual currents above the bottom layer moved towards the northeast.

The residual currents were weak during winter, and the vertical average of current speeds was only 7.5 cm/s. The current speed on the bottom was the lowest as 2.9 cm/s, whereas the current speed in the middle-upper layers (above the 34-m layer) fell generally consistently within the range of 8.0–9.0 cm/s. The residual current speeds during spring and neap tides were generally consistent in the vertical direction with an average speed of 6.0 cm/s during spring tides and 4.9 cm/s during neap tides. During winter, the residual currents shifted eastward toward the south, whereas the currents during the spring tides shifted eastward toward the south and the currents during neap tides shifted toward the east.

5 Discussion

5.1 *Runoff effects*

The runoff flux from the Changjiang River is large and exhibits seasonal variations (893×10^9 m^3/a. During 1951 to 2013, the runoff from May to October accounted for 70% of the annual flux). The expansion pattern of runoff is characterized by significant intra- and inter-seasonal variations (Lie et al., 2003), which significantly affect the flow field of the Changjiang Estuary. Our observations indicate that the residual currents during summer and autumn move northeastward with a high speed in the middle-upper layers (during summer and autumn, the average residual current speeds are 11.5 cm/s and 11.6 cm/s, respectively, in the 34-m layer), whereas during winter and spring, the residual currents generally move eastward during winter with a speed of only 7.5 cm/s. The implication is that this sea region is mainly controlled by the diluted Changjiang River discharge during summer and autumn. Runoff flux is one of the primary factors controlling the expansion and direction turning of the diluted water during the flood season (Le, 1984; Zhao, 1991), and the diluted Changjiang River discharge expands northeastward at 122°10′–122°30′E (Zhao, 1991; Zhou et al., 2009), with a critical runoff of 3.6×10^4–4.0×10^4 m^3/s. In our study, the Changjiang runoff was measured at Station Datong, and it took approximately 20 d for the runoff at Station Datong to reach the offshore region of the Changjiang Estuary (Wang et al., 2014, see below). Accordingly, the statistical runoff times were reduced by 20 d. In 2007, the freshwater discharge from the Changjiang River reached 4.9×10^4 m^3/s during summer and 1.9×10^4 m^3/s during autumn. Thus, the large amount of runoff originating from the Changjiang River during summer might be the primary contributor to the appearance of high-speed northeastward residual currents in this sea region. The runoff flux of the Changjiang River during winter is 1.0×10^4 m^3/s. The diluted water expands southward along the coast under the influence of the Coriolis force and northerly monsoon so that its effects could be neglected on this sea region.

The surface salinity observed by the buoy in this study provides independent supports for the effect of diluted Changjiang River discharge, as the average salinity on the surface (the 1.2-m layer) was 33.9 during the winter of 2010 whereas only 20.7 during summer. Wang et al. (2015) studied the characteristics of water flux and water body exchange in the Changjiang Estuary and surrounding water regions and similarly found that water apparently flows toward the sea region east of 123°E during summer.

5.2 *Effects of the Taiwan Warm Current on the offshore currents*

As a typical monsoon circulation current, the Taiwan Warm Current flows northeastward offshore of Zhejiang and Fujian Provinces toward the region south of the Changjiang Estuary. In winter, the current moves southward under the impacts of northerly winds in the water surface. No significant variations were found for the current directions in all layers for the rest of the year, which flow northward along the 50- to 100-m isobaths steadily. The current is stronger during summer and weaker during winter with a common speed of 15–40 cm/s, which, however, gradually decreases to 10–20 cm/s when the current reaches the diluted Changjiang River discharge far from shore (Guan, 1978; Su and Pan, 1989).

The vertical profiles of the current speeds during summer and autumn show significant outward convex shapes (especially during spring tides). The maximum current speed occurs in the middle layer while the residual current has the same characteristics and flows northward. The Taiwan Warm Current is most likely one of the main factors, aside from the diluted Changjiang River discharge, that causes such phenomena because, theoretically, the diluted Changjiang River discharge should significantly affect the surface and upper layers of water bodies. During summer, with high temperatures, salinity and density, the Taiwan Warm Current is very strong under the effects of southerly monsoons, reaching as far as 32°N. The invasion of the Taiwan Warm Current apparently speeds up and drags the middle layer at the observation station, leading to the increases in the speed of the current and residual current. Zhou et al. (2009) performed numerical simulations to study dynamic factors in the summer of 2006 and found that the invasion of the Kuroshio Current and its branches was relatively strong on the north side of the East China Sea so that it might be one of the dynamic factors that causes an increase in the current speed in the middle layer during summer and autumn. During winter, the Taiwan Warm Current weakens because of the strong effects of norther monsoons and thus exerts an accordingly weak effect on the offshore region. A vertical increase in current speeds does not occur in the middle layer during winter and the residual current moves southward with a

low speed.

5.3 *Effects of winds and tides on offshore currents*

Winds significantly affect the expansion of the diluted Changjiang River discharge (Liu et al., 2013). The top layer of the sea current in this study is the 10-m layer. Given that winds merely affect the surface layer (<10 m), apparent extreme weather was not observed during the observation period (Fig. 8), with northern and southern winds dominating during winter and summer, with average speeds of 8.2 m/s and 6.9 m/s, respectively. As a result, significant effects on the current speed or direction were not observed in this sea region.

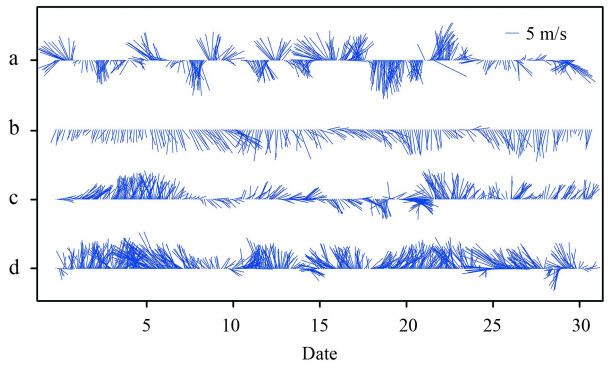

Fig. 8. Wind vectors plotted during different observation periods. a. Spring, April; b. summer, July; c. autumn, October; and d. winter, January.

Although the observation station is far from the mainland (approximately 150 km), the tidal force was still strong thanks to the large tidal range in this region. Apparent periodic variations occurred under the impact of spring and neap tides in all layers. The average current speeds during spring tides were approximately 1.7 to 3.0 times those during neap tides and the residual current speeds during spring tides were over 1.5 times those during neap tides. The residual currents during autumn were dominated by spring tides (vertical average of 19.4 cm/s), whereas those during neap tides were weak, indicating that the great influence of tides on this region.

6 Conclusions

Based on one-year continuous observations of sea currents using a large buoy in the sea region of the Changjiang Estuary, we demonstrated fixed-point sea current observation as an effective method to study the offshore currents. Based on our results, the following conclusions were drawn for the offshore region of the Changjiang Estuary.

(1) Sea currents rotate in a clockwise direction. In vertical direction, the directions of currents are consistent with minor seasonal variations.

(2) The shelf currents are relatively strong with trivial seasonal variations. In general, the average current speed in the middle-upper layer is approximately three times that in the bottom. Except the bottom layer, the current speeds are strongest during summer and weakest during winter. The average current speed during spring tides is strongest during autumn and weakest during winter. The average current speed during neap tides is strongest during summer and weakest during autumn.

(3) The average residual current speed ranges from 7.5 to 11.3 cm/s with the strongest speed appearing during summer and weakest during winter. In all layers within the water column, the residual currents during spring and winter move eastward, and the current direction shifts northeastward during summer and northward in autumn.

(4) The sea currents are constrained by the diluted Changjiang River discharge, the Taiwan Warm Current, monsoons and tides. Significant outward convex shapes are identified for the vertical profiles of current speeds during summer and autumn (in particular, during spring tides). The current speed in the middle layer is the highest and the residual currents show the same pattern of flowing towards the north. When the residual currents flow southwards with a relatively low speed, the current speed does not increase in the middle layer during winter.

References

Chang P H, Isobe A, Kang K R, et al. 2014. Summer behavior of the Changjiang diluted water to the East/Japan Sea: a modeling study in 2003. Continental Shelf Research, 81: 7–18

Chen Jiyu, Shen Huanting, Yun Caixing, et al. 1988. Processes of Dynamics and Geomorphology of the Changjiang Estuary (in Chinese). Shanghai: Shanghai Scientific and Technical Publishers, 48–62

Chen Xiaoyao, Wang Xiuhong, Guo Jingsong. 2006. Seasonal variability of the sea surface salinity in the East China Sea during 1990–2002. Journal of Geophysical Research, 111(C5): C05008, doi: 10.1029/2005jc003078

Dai Zhijun, Chu Ao, Stive M, et al. 2011a. Unusual salinity conditions in the Yangtze Estuary in 2006: impacts of an extreme drought or of the Three Gorges Dam. AMBIO, 40(5): 496–505

Dai Zhijun, Du Jinzhou, Chu Ao, et al. 2011b. Sediment characteristics in the North Branch of the Yangtze Estuary based on radioisotope tracers. Environmental Earth Sciences, 62(8): 1629–1634

Dai Zhijun, Du Jinzhou, Li Jiufa, et al. 2008. Runoff characteristics of the Changjiang River during 2006: effect of extreme drought and the impounding of the Three Gorges Dam. Geophysical Research Letters, 35(7): L07406, doi: 10.1029/2008GL033456

Dai Zhijun, Du Jinzhou, Zhang Xiaoling, et al. 2010. Variation of riverine material loads and environmental consequences on the Changjiang (Yangtze) estuary in recent decades (1955–2008). Environmental Science & Technology, 45(1): 223–227

Guan Bingxian. 1978. A summary of current system in the East China Sea (in Chinese) [dissertation]. Qingdao: Institute of Oceanology, Chinese Academy of Sciences, 126–183

Huang Y, Yin Baoshu, Perrie W, et al. 2008. Responses of summer time extreme wave heights to local climate variations in the East China Sea. Journal of Geophysical Research, 113(C9): C09031

Isobe A, Ando M, Watanabe T, et al. 2002. Freshwater and temperature transports through the Tsushima-Korea Straits. Journal of Geophysical Research, 107(C7): 3065, doi: 10.1029/2000JC000702

Kim H C, Yamaguch H, Yoo S, et al. 2009. Distribution of Changjiang diluted water detected by satellite chlorophyll-*a* and its interannual variation during 1998–2007. Journal of Oceanography, 65(1): 129–135

Le Kentang. 1984. A preliminary study of the path of the Changjiang diluted water: I. Model. Oceanologia et Limnologia Sinica (in Chinese), 15(2): 157–167

Li Daoji, Zhang Jing, Huang Daji, et al. 2002. Oxygen depletion off the Changjiang (Yangtze River) estuary. Science in China Series D: Earth Sciences, 45(12): 1137–1146

Liao Qiyu, Guo Binghuo, Liu Zanpei. 2001. Analysis of direction change mechanism of the Changjiang river diluted water in summer. Journal of Oceanography of Huanghai & Bohai Seas (in Chinese), 19(3): 19–25

Lie H J, Cho C H, Lee J H, et al. 2003. Structure and eastward extension of the Changjiang River plume in the East China Sea. Journal of Geophysical Research, 108(C3): 3077

Liu Baochao, Li Jianping, Feng Licheng. 2013. A modeling study of the effect of wind on Changjiang (Yangtze) River diluted water in summer. Haiyang Xuebao (in Chinese), 35(1): 25–37

Mao Hanli, Gan ZiJun, Lan Shufang. 1963. A preliminary study of the Yangtze diluted water and its mixing processes. Oceanologia et Limnologia Sinica (in Chinese), 5(3): 183–206

Moon J H, Pang I C, Yoon J H. 2009. Response of the Changjiang diluted water around Jeju Island to external forcings: a modeling study of 2002 and 2006. Continental Shelf Research, 29(13): 1549–1564

Park T, Jang C J, Jungclaus J H, et al. 2011. Effects of the Changjiang River discharge on sea surface warming in the Yellow and East China Seas in summer. Continental Shelf Research, 31(1): 15–22

Pu Yongxiu, Hang Weigeng, Xu Jianping. 2002. The spreading direction change of the Changjiang River diluted water in 7~10 days. Donghai Marine Science (in Chinese), 20(2): 1–5

Rabouille C, Conley D J, Dai M H, et al. 2008. Comparison of hypoxia among four river-dominated ocean margins: the Changjiang (Yangtze), Mississippi, Pearl, and Rhône rivers. Continental Shelf Research, 28(12): 1527–1537

Senjyu T, Enomoto H, Matsuno T, et al. 2006. Interannual salinity variations in the Tsushima Strait and its relation to the Changjiang discharge. Journal of Oceanography, 62(5): 681–692

Su Jilan. 2005. Zhongguo Jinhai Shuiwen (in Chinese). Beijing: China Ocean Press, 229–249

Su Jilan, Pan Yuqiu. 1989. A preliminary study of shelf circulation dynamics north of Taiwan. Haiyang Xuebao (in Chinese), 11(1): 1–14

Tang Jun, Shen Yongming, Qiu Dahong. 2008. Numerical simulation of longshore currents and pollutant movement in waves and currents in coastal zone. Haiyang Xuebao (in Chinese), 30(1): 147–155

Wang Ya, He Qing, Shen Jian. 2014. The study of the transport timescale in the Changjiang Estuary. Haiyang Xuebao (in Chinese), 36(1): 45–55

Wang Xiaohong, Yu Zhiming, Fan Wei, et al. 2015. Water flux and exchange in Changjiang River estuary and adjacent waters on coupled model of hydrodynamic roms and box model. Oceanologia et Limnologia Sinica (in Chinese), 46(1): 118–132

Wen Wei, Chang Yuanpin, Dai Zhijun. 2014. Streamflow changes of the Changjiang (Yangtze) River in the recent 60 years: impacts of the East Asian summer monsoon, ENSO, and human activities. Quaternary International, 336: 98–107

Wu Hui, Shen Jian, Zhu Jianrong, et al. 2014. Characteristics of the Changjiang plume and its extension along the Jiangsu Coast. Continental Shelf Research, 76: 108–123

Zhang Wenjing, Zhu Shouxian, Li Xunqiang, et al. 2014. Impact of tide induced residual current and tidal mixing on the low salinity water lens in the northeast out of the Changjiang Estuary. Haiyang Xuebao (in Chinese), 36(3): 9–18

Zhao Baoren. 1991. Mechanism of expansion trend of the Yangtze diluted water. Haiyang Xuebao (in Chinese), 13(5): 600–610

Zhao Baoren. 1993. The upwelling off Yangtze River estuary. Haiyang Xuebao (in Chinese), 15(2): 108–114

Zhou Feng, Xuan Jiliang, Ni Xiaobo, et al. 2009. A preliminary study on variations of the Changjiang Diluted Water between August 1999 and 2006. Haiyang Xuebao (in Chinese), 31(4): 1–12

Zhu Jianrong, Hu Dunxin, Xiao Chengyou. 2004a. Observed residual currents off the Changjiang (Yangtze) River mouth in winter time of 1959 and 1982. Chinese Journal of Oceanology and Limnology, 22(3): 244–249

Zhu Jianrong, Qi Dingman, Xiao Chengyou. 2004b. Observed residual currents off the Changjiang (Yangtze) River mouth in summer time of 1959 and 1982. Chinese Journal of Oceanology and Limnology, 22(3): 250–255

Zhu Jianrong, Shen Huanting, Zhou Jian. 1997. Numerical simulation of the impact of the Subei Coastal Current on the expansion of the Changjiang River diluted water in summer. Journal of East China Normal University (Natural Science) (in Chinese), (2): 62–67

Zhu Jianrong, Wang Jinhui, Shen Huanting, et al. 2005. Observation and analysis of the diluted water and red tide in the sea off the Changjiang River mouth in middle and late June 2003. Chinese Science Bulletin, 50(3): 240–247

Zhu Jianrong, Xiao Chengyou, Shen Huanting. 1998. Numerical model simulation of expansion of Changjiang diluted water in summer. Haiyang Xuebao (in Chinese), 20(5): 13–22